IDENTIFICATION OF NONLINEAR VIBRATING STRUCTURES BY POLYNOMIAL EXPANSION IN THE Z-DOMAIN

Alessandro Fasana, Luigi Garibaldi, Stefano Marchesiello

Politecnico di Torino, Dipartimento di Ingegneria Meccanica e Aerospaziale – DIMEAS
Corso Duca degli Abruzzi, 24, I-10129 Torino Italy

https://doi.org/10.1016/j.ymssp.2015.11.021

Cite as:

Fasana Alessandro, Garibaldi Luigi, Marchesiello Stefano (2017). Identification of nonlinear vibrating structures by polynomial expansion in the z-domain. MECHANICAL SYSTEMS AND SIGNAL PROCESSING, vol. 84, p. 21-33, ISSN: 0888-3270, doi: dx.doi.org/10.1016/j.ymssp.2015.11.021

IDENTIFICATION OF NONLINEAR VIBRATING STRUCTURES BY POLYNOMIAL EXPANSION IN THE *Z*-DOMAIN

Alessandro Fasana, Luigi Garibaldi, Stefano Marchesiello

Politecnico di Torino

Dipartimento di Ingegneria Meccanica e Aerospaziale – DIMEAS

Corso Duca degli Abruzzi, 24, I-10129 Torino Italy

Tel.: +39 011 0903397; fax: +39 011 0906999.

E-mail address: alessandro.fasana@polito.it

Keywords: Linear and nonlinear identification; frequency domain; *z*-transform; MDOF system.

Abstract

A new method in the frequency domain for the identification of nonlinear vibrating structures is described, by adopting the perspective of nonlinearities as internal feedback forces. The technique is based on a polynomial expansion representation of the frequency response function of the underlying linear system, relying on a *z*-domain formulation. A least squares approach is adopted to take into account the information of all the frequency response functions but, when large data sets are used, the solution of the resulting system of algebraic linear equations can be a difficult task. A procedure to drastically reduce the matrix dimensions and consequently the computational cost – which largely depends on the number of spectral lines – is adopted, leading to a compact and well conditioned problem. The robustness and numerical performances of the method are demonstrated by its implementation on simulated data from single and two degree of freedom systems with typical nonlinear characteristics.

1. Introduction

The research activity in the wide field of nonlinear system dynamics is attested by the continuous publication of numerous books, PhD theses, papers and benchmarks – see for example [1-9]. In particular the nonlinear system identification, just like the sector of modal parameters extraction, exhibits a sort of time–frequency ambivalence. As an example, a time-domain subspace identification algorithm, extended to nonlinear system and named nonlinear subspace identification (NSI), was proposed in [10] and later developed in the frequency domain in [11]. Each implementation has advantages and disadvantages as pointed out in [12], so that it should be advisable to rely on different data processing techniques to investigate structures properties. The objective of the present paper is to present a new frequency domain method for the identification of

nonlinear systems, inspired by the basic principle of the nonlinear identification through feedback of the outputs (NIFO) technique introduced in [13]. Each frequency response function (FRF) of the underlying linear system is expressed by a polynomial ratio in the *z*-domain, shifting the problem from the estimation of the FRFs to the definition of the constant coefficients describing both the linear and nonlinear parts of the system. Poles and zeros of the various FRFs are in other words simultaneously computed with the (assumed frequency independent) parameters characterizing the nonlinear terms, thus achieving a complete identification of the structure in the same step of the procedure. The nonlinear identification by polynomial expansion in the *z*-domain (NIPEZ) method here proposed can deal with multiple input multiple output (MIMO) systems containing different and (possibly) many nonlinearities and is designed in order to efficiently compute a least squares solution, which takes into account the information contained in each FRF.

The paper is organized as follows. Section 2 introduces the theoretical background of the NIPEZ method, describing the procedure in details. Section 3 is devoted to the numerical examples, with single and two degree of freedom systems. Synthetic data sets are corrupted by additive noise to show its influence on estimates of linear and nonlinear parameters. Stabilisation diagrams are used for validating the identification procedure. The conclusions of the study are presented in Section 4.

2. Outline of the method

For a time invariant, viscously damped system with *N* degrees of freedom and *S* nonlinearities, the second order time domain equations of motion can be written in the form [13]

$$\mathbf{M}\ddot{\mathbf{x}}(t)+\mathbf{C}\dot{\mathbf{x}}(t)+\mathbf{K}\mathbf{x}(t)=\mathbf{f}(t)+\sum_{s=1}^{S}\mathbf{L}_s\mu_s g_s(t) \tag{1}$$

where **M**, **C**, **K** are symmetric square matrices, **x**(t) is the displacement column vector, **f**(t) is the external forces column vector, $g_s(t)$ indicates the kind of nonlinearity and has to be specified *a priori*, μ_s is the constant parameter of the nonlinear term and vector $\mathbf{L}_s$ specifies its position, with $\mathbf{L}_s=\begin{bmatrix} L_{1s} & \cdots & L_{ks} & \cdots & L_{Ns} \end{bmatrix}^T$ and $L_{ks}=0$ or $L_{ks}=\pm 1$. In this model any nonlinear contribution is acting as a force whose position and form is entirely defined, while its intensity depends on the unknown constants μ_s.

It's worth noticing that the methodology relies on the feedback of the outputs stated by eq.(1): the same principle has been used in [10, 11, 13] which can therefore be assumed as valuable terms of comparison.

The frequency domain model corresponding to eq. (1) is

$$\mathbf{B}_L(\omega)\mathbf{X}(\omega) = \mathbf{F}(\omega) + \sum_{s=1}^{S} \mathbf{L}_s \mu_s G_s(\omega) \tag{2}$$

where $\mathbf{B}_L(\omega)$ is the linear impedance matrix and $\mathbf{X}(\omega)$, $\mathbf{F}(\omega)$, $G_s(\omega)$ are the Fourier transforms of **x**(t), **f**(t) and $g_s(t)$ respectively – $\mathbf{L}_s$ and μ_s are constant quantities. In particular it is assumed that the nonlinear terms μ_s do not vary with frequency, which distinguishes the NIPEZ method from both NIFO and NSI techniques [13, 10].

With the position $\mathbf{H}(\omega) = \mathbf{B}_L^{-1}(\omega)$, where $\mathbf{H}(\omega)$ is the (linear) frequency response matrix, eq. (2) becomes

$$\mathbf{X}(\omega) = \mathbf{H}(\omega)\mathbf{F}(\omega) + \sum_{s=1}^{S} \mathbf{H}(\omega)\mathbf{L}_s \mu_s G_s(\omega) \tag{3}$$

which represents the structure of the identification model.

The input and output time histories (appropriately sampled and sufficiently long), the number, kind and position of the nonlinearities are given so that $\mathbf{X}(\omega)$, $\mathbf{F}(\omega)$, $\mathbf{L}_s$ and $G_s(\omega)$ are completely defined.

The question is how the modal parameters (frequency, damping ratio and mode shape, all of them buried in the FRF matrix $\mathbf{H}(\omega)$) of the underlying linear system as well as the μ_s parameters of the nonlinear terms can be extracted.

To explain the proposed NIPEZ procedure we firstly focus the attention on the single input F_p single output X_q (SISO) equation, extracted from eq. (3) – ω is removed for the sake of simplicity:

$$X_q = H_{qp}F_p + \left(\sum_{s=1}^{S} \mathbf{H}\, \mathbf{L}_s \mu_s G_s \right)_q \tag{4}$$

or also, in an expanded notation

$$X_q = H_{qp}F_p + \mu_1 G_1 \sum_{k=1}^{N} H_{qk}\, L_{k1} + \square \; + \mu_S G_S \sum_{k=1}^{N} H_{qk}\, L_{kS} \tag{5}$$

Lacking the nonlinear terms, eq. (5) would give $X_q = H_{qp}F_p$ as expected. This also reminds us that a sound computation of a FRF, i.e. H_{qp}, is better achieved by adopting one of the usual estimators based on power spectral density (PSD) functions [14] than by simply performing the ratio X_q / F_p.

It is then advisable to multiply eq.(5) by the complex conjugate output X_q^* so to pave the way for the computation of PSD functions by means of the Welch periodogram:

$$X_q^* X_q = H_{qp}X_q^* F_p + \mu_1 X_q^* G_1 \sum_{k=1}^{N} H_{qk}\, L_{k1} + \square \; + \mu_S X_q^* G_S \sum_{k=1}^{N} H_{qk}\, L_{kS} \tag{6}$$

A rational fraction expression is then assumed for the FRF, based on the *z*-transform of the linear system impulse response function [15]

$$H_{qp} = \frac{N_{qp}}{D} = \frac{\left(b_1 z + \cdots + b_{2n} z^{2n}\right)_{qp}}{a_0 + a_1 z + \cdots + a_{2n-1} z^{2n-1} + z^{2n}} \tag{7}$$

where $z = e^{j\omega\Delta t}$, Δt is the sampling period, $f_s = 1/\Delta t$ is the sampling frequency and $2n$ is the order of the model, theoretically equal to twice the number of degrees of freedom N of the system.

Eq.(7) corresponds to a common denominator model [16, 17] so that numerator N_{qp}, and consequently the zeros of the FRF, varies with the input p and the output q whilst denominator D, and consequently the poles of the system, remains unchanged. Substituting eq.(7) into eq. (6) gives

$$X_q^* X_q D = N_{qp} X_q^* F_p + \mu_1 X_q^* G_1 \sum_{k=1}^{N} N_{qk} L_{k1} + \cdots + \mu_S X_q^* G_S \sum_{k=1}^{N} N_{qk} L_{kS} \tag{8}$$

and then

$$\begin{bmatrix} z^0 & \cdots & z^{2n-1} \end{bmatrix} X_q^* X_q \mathbf{a} + z^{2n} X_q^* X_q = \begin{bmatrix} z^1 & \cdots & z^{2n} \end{bmatrix} X_q^* F_p \, \mathbf{b}_{qp} +$$

$$+ \mu_1 X_q^* G_1 \sum_{k=1}^{N} \begin{bmatrix} z^1 & \cdots & z^{2n} \end{bmatrix} \mathbf{b}_{qk} L_{k1} + \cdots + \mu_S X_q^* G_S \sum_{k=1}^{N} \begin{bmatrix} z^1 & \cdots & z^{2n} \end{bmatrix} \mathbf{b}_{qk} L_{kS} \tag{9}$$

where $\mathbf{a} = \begin{bmatrix} a_0 & a_1 & \cdots & a_{2n-1} \end{bmatrix}^T$ and $\mathbf{b}_{qp} = \begin{bmatrix} b_1 & b_2 & \cdots & b_{2n} \end{bmatrix}_{qp}^T$

The sums on the right hand side can be assembled into new vectors $\mathbf{d}_{qs}$ so that eq.(9) boils down to

$$\begin{bmatrix} z^0 & \cdots & z^{2n-1} \end{bmatrix} S_{XqXq} \mathbf{a} + z^{2n} S_{XqXq} = \begin{bmatrix} z^1 & \cdots & z^{2n} \end{bmatrix} S_{XqFp} \, \mathbf{b}_{qp} + \begin{bmatrix} z^1 & \cdots & z^{2n} \end{bmatrix} \sum_{s=1}^{S} S_{XsGs} \mathbf{d}_{qs} \tag{10}$$

with S_{XqXq}, S_{XqFp} and S_{XsGs} indicating auto and cross power spectral densities (PSD) and

$$\mathbf{d}_{qs} = \mu_s \sum_{k=1}^{N} \mathbf{b}_{qk} L_{ks} \tag{11}$$

Eq.(10) has been written for a single spectral line, i.e. for $z = e^{j\omega\Delta t}$, but may be repeated for every frequency ω so as to obtain a set of M equations, M being the number of spectral lines in exam. In matrix form

$$\mathbf{A}_q \mathbf{a} + \mathbf{n}_q + \mathbf{B}_{qp} \, \mathbf{b}_{qp} + \sum_{s=1}^{S} \mathbf{D}_{qs} \mathbf{d}_{qs} = \mathbf{e}_q \tag{12}$$

where $\mathbf{n}_q \in \mathbf{C}^{M\times 1}$ is the known vector, $\mathbf{e}_q \in \mathbf{C}^{M\times 1}$ is the error vector and matrices $\mathbf{A}_q \in \mathbf{C}^{M\times 2n}$, $\mathbf{B}_{qp} \in \mathbf{C}^{M\times 2n}$ and $\mathbf{D}_{qs} \in \mathbf{C}^{M\times 2n}$ are defined according to the elements in eq.(10).

Eq.(12) links the linear ($\mathbf{a}$ and $\mathbf{b}_{qp}$) and nonlinear ($\mathbf{d}_{qs}$) vectors of a SISO system and drives

straight to the following multiple input single output –MISO– formulation

$$\mathbf{A}_q\mathbf{a}+\sum_{p=1}^{P}\mathbf{B}_{qp}\,\mathbf{b}_{qp}+\sum_{s=1}^{S}\mathbf{D}_{qs}\mathbf{d}_{qs}+\mathbf{n}_q=\mathbf{e}_q \tag{13}$$

P being the number of inputs.

Finally a multiple input multiple output –MIMO– expression is found directly from eq.(13)

$$\begin{cases} \mathbf{A}_1\mathbf{a}+\sum_{p=1}^{P}\mathbf{B}_{1p}\,\mathbf{b}_{1p}+\sum_{s=1}^{S}\mathbf{D}_{1s}\mathbf{d}_{1s}+\mathbf{n}_1=\mathbf{e}_1 \\ \vdots \\ \mathbf{A}_Q\mathbf{a}+\sum_{p=1}^{P}\mathbf{B}_{Qp}\,\mathbf{b}_{Qp}+\sum_{s=1}^{S}\mathbf{D}_{Qs}\mathbf{d}_{Qs}+\mathbf{n}_Q=\mathbf{e}_Q \end{cases} \tag{14}$$

with $q = 1,\ldots,Q$, Q being the number of outputs.

The total number of unknown real constants, pertaining to $\mathbf{a}$, $\mathbf{b}_{qp}$ and $\mathbf{d}_{qs}$, is $2n+2n\cdot P\cdot Q+2n\cdot S\cdot Q$ while the number of equation is $M\cdot Q$: the linear system of equations (14) can then be solved, by minimising the error vectors $\mathbf{e}_q$.

In order to obtain a reliable solution, an overdetermined system of equations is sought for and then the number of rows of eq.(14) should be at least equal to the number of columns. This last requirement is easily fulfilled by choosing a number of spectral lines M big enough: notice that this value can also be very large, depending on the initial calculation of the PSD functions. Unfortunately this approach is numerically not effective, because of the potentially huge number of complex-valued equations to be solved, even when few nonlinearities and degrees of freedom are involved. The development of an alternative least squares procedure is then well worth the quite cumbersome algebra briefly summarised as follows.

Let $E_q^2=\mathbf{e}_q^H\mathbf{e}_q$ be the real valued scalar error (^{H} indicates the Hermitian transpose), computed on the M spectral lines of output q as per eq.(13). The global error, taking into account all the outputs is

$$E^2=\sum_{q=1}^{Q}E_q^2 \tag{15}$$

The former quantity is minimised by setting

$$\begin{cases} \partial E^2/\partial\mathbf{a}=0 & \\ \partial E^2/\partial\mathbf{b}_{qp}=0 & \text{with} \quad p=1,\ldots,P \\ \partial E^2/\partial\mathbf{d}_{qs}=0 & \end{cases} \tag{16}$$

Tedious algebraic developments (Appendix A) lead to the compact expression

$$\mathbf{S}\mathbf{x}=\mathbf{m} \tag{17}$$

where **S** is a Hermitian matrix formed by a proper multiplication of $\mathbf{A}_q$, $\mathbf{B}_{qp}$ and $\mathbf{D}_{qs}$ matrices, **m** is the vector of known coefficients formed by $\mathbf{A}_q$, $\mathbf{B}_{qp}$, $\mathbf{D}_{qs}$and $\mathbf{n}_q$, **x** contains the real unknown vectors $\mathbf{a}$, $\mathbf{b}_{qp}$ and $\mathbf{d}_{qs}$– examples of the structure of **S**, **m** and **x** are given in the next section.

Eq.(17) is completely equivalent to eq.(14) but contains a reduced number of equation, i.e. $2n+2n\cdot P\cdot Q+2n\cdot S\cdot Q$, thus requiring a much lower computational effort. Its solution gives the coefficients **a** of the denominator of the FRF –eq.(7)– which in turn allow to compute the poles of the system; also vectors $\mathbf{b}_{qp}$ and $\mathbf{d}_{qs}$ are determined so that the nonlinear parameters μ_s can be identified by using eq.(11). It may be worth noticing that the solution of eq.(17) directly provides vectors $\mathbf{a}$ and $\mathbf{b}_{qp}$ that is, with a straightforward manipulation, natural frequencies, damping ratios and mode shapes of the linear system. The validation of the model, as indicated by the examples in the next section, is mainly based on a correct usage of stabilization diagrams of both linear and nonlinear parameters.

The proposed procedure can be summarized as follows:

1) measurement of the input and output time histories;
2) definition of a model based on **M**, **C**, **K** matrices and feedback of the outputs – eq.(1);
3) reformulation of the problem in the frequency domain – eq.(3);
4) choice of a rational fraction formulation, written in the *z*-domain, to describe the frequency response function of the underlying linear system – eq.(7);
5) definition of a least square procedure to minimize the error between the model and the measures – eqs.(14-17);
6) definition of the modal parameters (related to the linear underlying structure) and the nonlinear coefficients by exploiting the capabilities of stabilization diagrams.

It may be useful to notice that it is not possible to apply the proposed technique to calculate the outputs on the basis of given inputs and estimated linear and nonlinear parameters. In fact the method can not reconstruct matrices **M**, **C**, **K** but only the related modal parameters, in particular natural frequencies and damping ratios.

3. Numerical examples

Examples based on single and two degrees of freedom systems with different sort of nonlinearities are discussed in this section. They all are very similar to the test cases presented in [10] so to have a direct comparison with a well established but totally independent time domain algorithm. The proposed method proves numerically efficient, results are very good, and stabilisation diagrams reveal useful in choosing both the linear and nonlinear solutions.

The integration of all the following differential equations has been performed by a Runge-Kutta scheme, implemented in the Matlab® script ode45.

3.1 Example 1: single degree of freedom system with cubic stiffness

The first example of application for NIPEZ method is a most classical one: the single degree of freedom system with a cubic hardening stiffness. Its motion is described by the Duffing equation

$$m\ddot{x}(t)+c\dot{x}(t)+kx(t)+k_3x^3(t)=f(t) \tag{18}$$

whose parameters are listed in Table 1. The chosen excitation *f(t)* is a zero-mean Gaussian noise and the underlying linear system has natural frequency f_r=3.948 Hz and damping ratio ζ=3.10%

By comparing eq.(18) and eq.(1) it's obvious that $N=P=Q=S=1$, $\mathbf{L}_s \equiv \mathbf{L}_1 = L_{11} = -1$, $g_s(t) \equiv g_1(t) = x^3$ and $\mu_s \equiv \mu_1 = k_3$. Eq.(11) also is very simple and reads $\mathbf{d}_{11} = \mu_1 \mathbf{b}_{11}$ $L_{11} = -k_3 \mathbf{b}_{11}$

Auto and cross PSD, see eqs. (10) and (12), are computed by Welch periodogram method, with the parameters listed in Table 2.

Table 1

Parameters of the Duffing equation

m (kg)	*c* (Ns/m)	*k* (N/m)	k_3 (N/m^3)
1.3	2	800	$1.5 \cdot 10^6$

Table 2

Parameters for PSD estimation

Number of spectral lines *M*	Overlap (%)	Window	Number of time samples	Sampling frequency f_s (Hz)
4096	67	Hann	50000	100

Eq.(14) involves a single equation $\mathbf{A}_1\mathbf{a}+\mathbf{B}_{11}\,\mathbf{b}_{11}+\mathbf{D}_{11}\mathbf{d}_{11}+\mathbf{n}_1=\mathbf{e}_1$ and the least squares procedure outlined by eqs.(15-16) leads to the following square $(2n\cdot 3)\times(2n\cdot 3)$ system:

$$\begin{bmatrix} \mathbf{A}_1^H\mathbf{A}_1 & \mathbf{A}_1^H\mathbf{B}_{11} & \mathbf{A}_1^H\mathbf{D}_{11} \\ \mathbf{B}_{11}^H\mathbf{A}_1 & \mathbf{B}_{11}^H\mathbf{B}_{11} & \mathbf{B}_{11}^H\mathbf{D}_{11} \\ \mathbf{D}_{11}^H\mathbf{A}_1 & \mathbf{D}_{11}^H\mathbf{B}_{11} & \mathbf{D}_{11}^H\mathbf{D}_{11} \end{bmatrix} \begin{Bmatrix} \mathbf{a} \\ \mathbf{b}_{11} \\ \mathbf{d}_{11} \end{Bmatrix} = \begin{Bmatrix} -\mathbf{A}_1^H\mathbf{n}_1 \\ -\mathbf{B}_{11}^H\mathbf{n}_1 \\ -\mathbf{D}_{11}^H\mathbf{n}_1 \end{Bmatrix} \tag{19}$$

Figure 1 represents the $H_2(\omega)$ linear estimation of the FRF, based on the input and output time histories of the nonlinear Duffing oscillator. As expected the resonance band is right shifted with respect to the linear natural frequency f_r at about 4 Hz. The output has also been corrupted with Gaussian zero-mean noise, whose root mean square (rms) is 3% of the output rms, roughly corresponding to a 30dB signal-to-noise ratio. The effect of the noise is appreciable above 12 Hz whilst in the resonance region the magnitude of FRFs curves are almost equal.

The NIPEZ technique has been applied in both cases in the frequency range 0-8 Hz with model order $2n$ varying from 2 to 80, in order to highlight the importance of this parameter. The stabilisation diagram for the nonlinear stiffness k_3 is plotted in Figure 2, in the noisy condition. It is clear that a single degree of freedom model, corresponding to model order 2, is not sufficient to achieve an acceptable estimate of k_3, which is largely underestimated; on the contrary the identified frequency, related to the linear parameters, is only 5% higher than expected. The wrong approximation of the nonlinear parameter at the ideal model order, which is a weakness of the methodology and is indeed shared with other nonlinear identification techniques, highlights the importance of the stabilization diagram, as also proposed in [12], which is in fact very stable beyond $2n$=10 (Fig. 2). The mean value and the standard deviation of the linear parameters, f_1 and ζ_1, and nonlinear stiffness k_3 ($10<2n<80$) are reported in Table 3: the relative error on the nonlinear stiffness is below 0.5%. A very limited dispersion of data around the mean value is present, with a particularly low standard deviation when no noise is added. It is worth noticing that also the damping ratio is determined with high precision and low dispersion.

The same example is reported in [10] where the error on k_3 is particularly low without noise and increases to 1.62% in the 3% noise case.

Table 3: linear and nonlinear parameters of the Duffing equation estimated by NIPEZ method

	No noise			3% noise		
	k_3 (N/m^3)	f_1 (Hz)	ζ_1 (%)	k_3 (N/m^3)	f_1 (Hz)	ζ_1 (%)
Mean value	$1.5061 \cdot 10^6$	3.951	3.10	$1.5041 \cdot 10^6$	3.951	3.10
Standard deviation	$5.1 \cdot 10^2$	$4.16 \cdot 10^{-4}$	0.008	$2.23 \cdot 10^3$	$6.78 \cdot 10^{-4}$	0.022

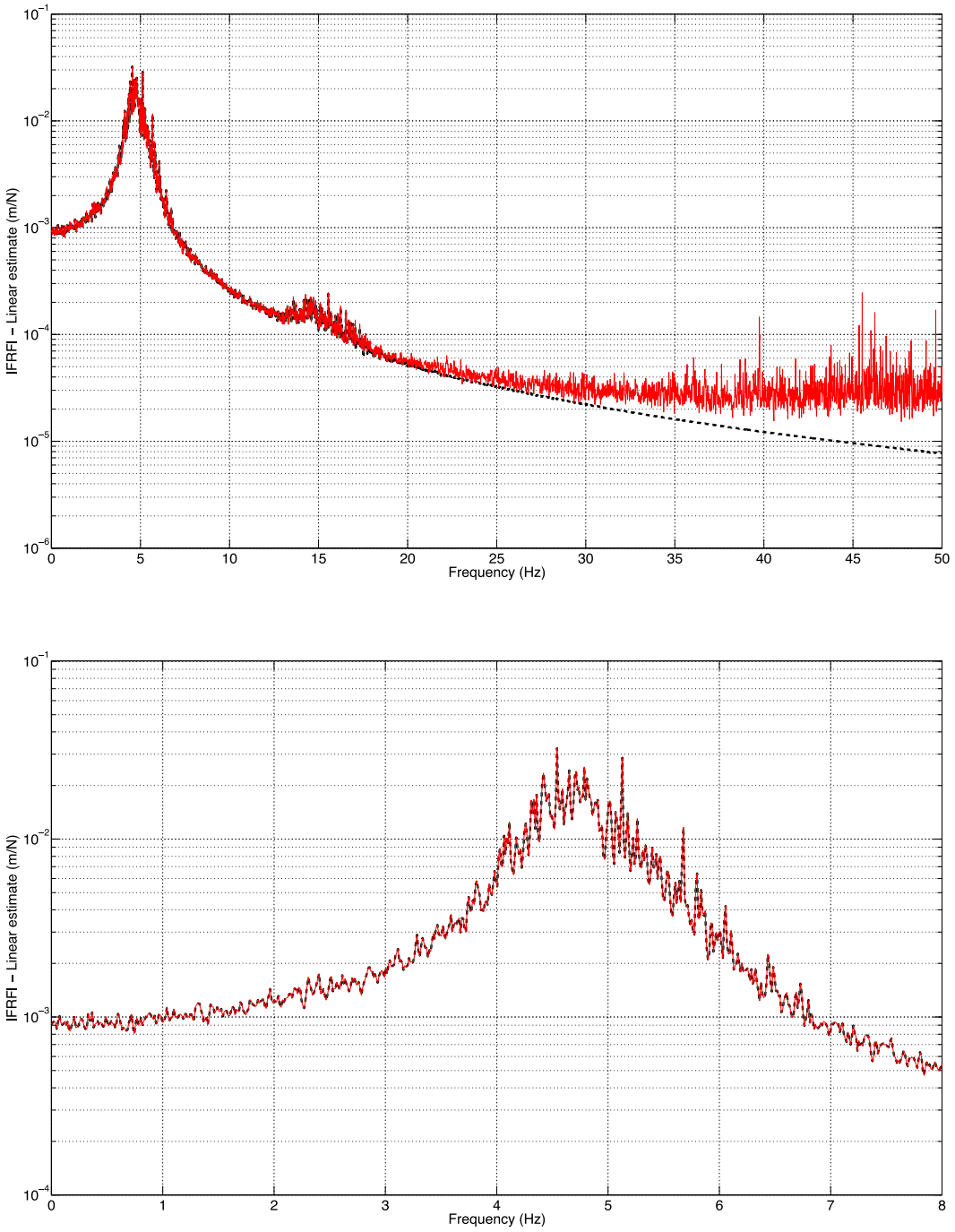

Figure 1: $H_2(\omega)$ linear estimate of the FRF of the Duffing oscillator, with (solid line) and without (dashed line) noise on output, with a zoom in the resonance band.

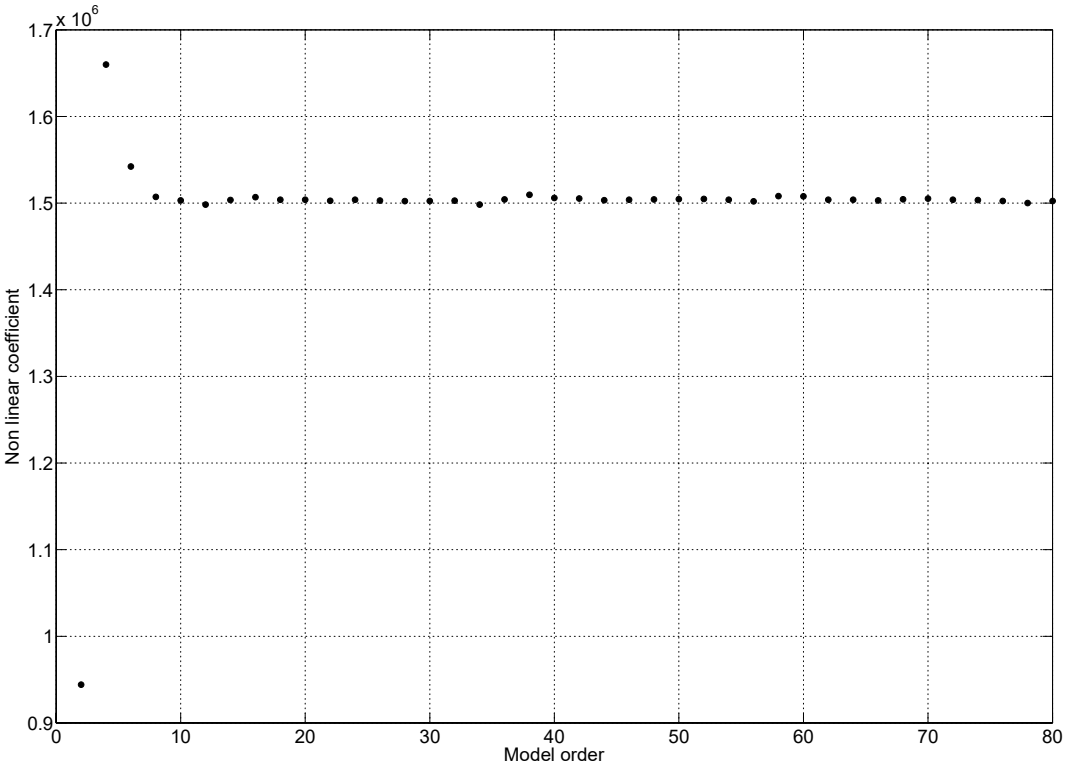

Figure 2: stabilisation diagram of the nonlinear stiffness coefficient k_3 (Duffing oscillator).

3.2 Example 2: single degree of freedom system with clearance

The second example is still dedicated to a SDOF system, with the same linear parameters as in Section 3.1, but with clearance type nonlinearity. The equation of motion is

$$m\ddot{x}(t) + c\dot{x}(t) + kx(t) + F_d(t) = f(t) \tag{20}$$

where

$$F_d(t) = 0 \qquad \text{for} \qquad |x| \le \mathrm{d}$$

$$F_d(t) = k_c\left(x - \mathrm{d}\,sgn(x)\right) \qquad \text{for} \qquad |x| > \mathrm{d}$$

d=0.01 m is the deadspace (clearance) and k_c=1000 N/m is the stiffness.

Also in this case the NIPEZ method has been applied in the frequency range 0-8 Hz with model order 2n varying from 2 to 80 (results are presented for noisy data only). Assuming d=0.01 m, the stabilisation diagram for the nonlinear stiffness k_c is similar to Figure 2 (except for the numerical values), and again model order 2 is not sufficient to achieve an acceptable estimate of the nonlinear parameter. A very stable diagram is obtained beyond 2n=10 leading to the mean value k_c=1.002 $\cdot 10^3$ N/m and standard deviation 1.52 N/m.

This is of course an ideal situation because the deadspace is usually unknown and has to be determined together with the stiffness k_c. The stabilisation diagram of coefficient k_c is of help also

in this case because when a wrong deadspace is selected, the standard deviation of the stiffness is much larger than in the correct case – Table 4. It is also worth mentioning that in this conditions the natural frequency f_r and damping ratio ζ not only are no more correctly estimated (which would be impossible to tell without a reference value) but also are quite variable with the model order, thus suggesting some drawback in the identification procedure.

Table 4: influence of the clearance length on the stiffness coefficient k_c.

d (m)	0.007	0.008	0.009	0.010	0.011	0.012	0.013
k_c mean value (N/m)	829.5	886.7	942.8	1002	1057	1105	1142
k_c standard deviation (N/m)	55.8	34.8	14.5	1.52	8.24	29.8	43.9

3.3 Example 3: single degree of freedom system with polynomial nonlinearity

The third example is still dedicated to a SDOF system, with the same linear parameters as in Section 3.1, but with a polynomial expression of the nonlinearity in the form

$$F_p(t) = k_2 x^2(t) + k_3 x^3(t) + k_4 x^4(t) + k_5 x^5(t) + k_6 x^6(t) + k_7 x^7(t) \tag{21}$$

Six μ_s constant parameters of the nonlinear term – $\mu_1 = k_2$, …, $\mu_6 = k_7$ – are to be found and the dimensions of matrix **S** – eq.(17) – increase accordingly. For the sake of brevity eq.(17) is expanded for two terms only:

$$\begin{bmatrix} \mathbf{A}_1^H\mathbf{A}_1 & \mathbf{A}_1^H\mathbf{B}_{11} & \mathbf{A}_1^H\mathbf{D}_{11} & \mathbf{A}_1^H\mathbf{D}_{12} \\ \mathbf{B}_{11}^H\mathbf{A}_1 & \mathbf{B}_{11}^H\mathbf{B}_{11} & \mathbf{B}_{11}^H\mathbf{D}_{11} & \mathbf{B}_{11}^H\mathbf{D}_{12} \\ \mathbf{D}_{11}^H\mathbf{A}_1 & \mathbf{D}_{11}^H\mathbf{B}_{11} & \mathbf{D}_{11}^H\mathbf{D}_{11} & \mathbf{D}_{11}^H\mathbf{D}_{12} \\ \mathbf{D}_{12}^H\mathbf{A}_1 & \mathbf{D}_{12}^H\mathbf{B}_{11} & \mathbf{D}_{12}^H\mathbf{D}_{11} & \mathbf{D}_{12}^H\mathbf{D}_{12} \end{bmatrix} \begin{Bmatrix} \mathbf{a} \\ \mathbf{b}_{11} \\ \mathbf{d}_{11} \\ \mathbf{d}_{12} \end{Bmatrix} = \begin{Bmatrix} -\mathbf{A}_1^H\mathbf{n}_1 \\ -\mathbf{B}_{11}^H\mathbf{n}_1 \\ -\mathbf{D}_{11}^H\mathbf{n}_1 \\ -\mathbf{D}_{12}^H\mathbf{n}_1 \end{Bmatrix} \tag{22}$$

with $\mathbf{d}_{11} = \mu_1\mathbf{b}_{11}$ $L_{11} = -k_2\mathbf{b}_{11}$ and $\mathbf{d}_{12} = \mu_2\mathbf{b}_{11}$ $L_{12} = -k_3\mathbf{b}_{11}$, but the same structure applies to any similar expansion. It must be stressed that it is not possible to incorporate a linear term in the polynomial expression (21), because its contribution would mix with the linear term $kx(t)$: in the identification procedure it would consequently be impossible to tell which is which.

The results, again with model order up to 80 and noisy data, are summarised in Table 5 where the nonlinear stiffness constants and their standard deviations are reported. In the equation of motion k_3 and k_5 only have been set different from zero, and in fact coefficients k_2 - k_4 - k_6 - k_7 exhibit standard deviations of the same order of their mean values (or even larger), thus revealing not to be reliable at all. The remaining terms k_3 and k_5 do not exactly match the actual values but can still copy with good accuracy the nonlinear force. In Figure 3 the dashed line representing the nonlinear original

force – eq.(21) – is almost overlaid on the solid line representing the force reconstructed by using the coefficients reported in Table 5.

Good approximation is reached also for the linear parameters: the natural frequency is 3.937 Hz (standard deviation: 0.0056 Hz) and the damping ratio is 3.08 % (standard deviation: 0.08%).

Table 5: coefficients of the polynomial stiffness.

	k_2 (N/m^2)	k_3 (N/m^3)	k_4 (N/m^4)	k_5 (N/m^5)	k_6 (N/m^6)	k_7 (N/m^7)
Ideal value	0	$1.00 \cdot 10^5$	0	$1.00 \cdot 10^8$	0	0
Mean value	106	$9.42 \cdot 10^4$	$-2.03 \cdot 10^5$	$1.17 \cdot 10^8$	$6.47 \cdot 10^7$	$-7.45 \cdot 10^9$
Standard deviation	56	$3.07 \cdot 10^3$	$1.30 \cdot 10^5$	$5.49 \cdot 10^6$	$1.08 \cdot 10^8$	$2.64 \cdot 10^9$

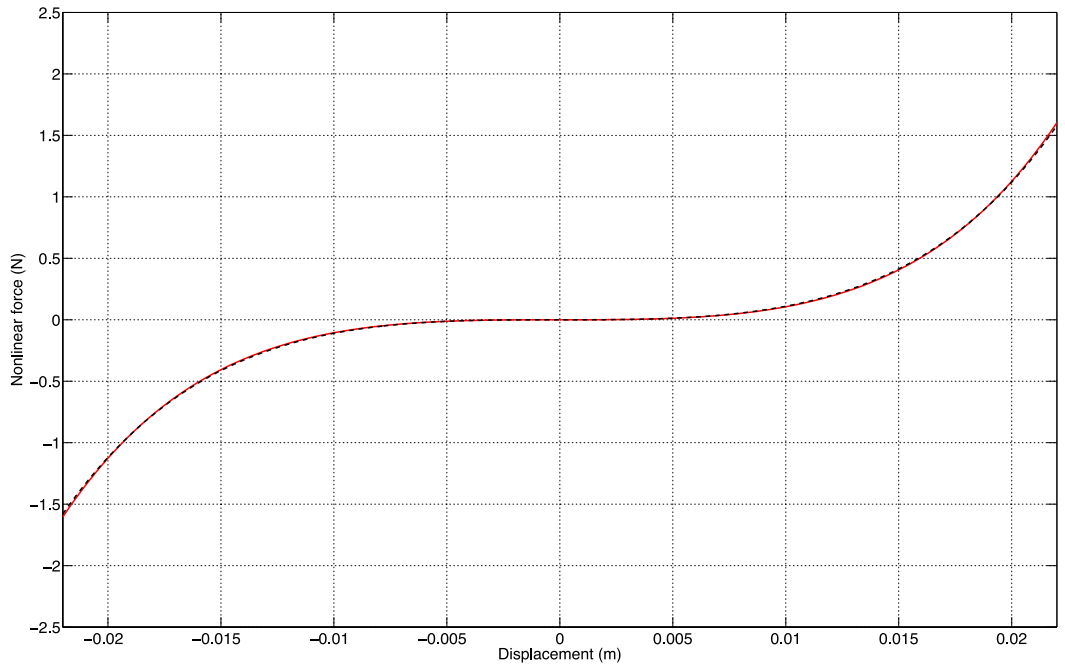

Figure 3: the original nonlinear polynomial force (dashed line) and its fitting (solid line).

On the basis of these results it could be advisable to limit the survey to the couple of stable nonlinear parameters only, the others being discarded. Estimates and variances would in fact improve to $k_3 = 1.006 \cdot 10^5$ N/m^3 (standard deviation $9.68 \cdot 10^2$ N/m^3) and $k_5 = 1.023 \cdot 10^8$ N/m^5 (standard deviation $1.00 \cdot 10^6$ N/m^5).

3.4 Example 4: two degrees of freedom system with three nonlinearities

A two degrees of freedom system with three nonlinear elements (Fig. 4), whose parameters are listed in Table 6, is the focus of this example. The last term of eq.(1) is

$$\sum_{s=1}^{S} \mathbf{L}_s \mu_s g_s(t) = \left\{ \begin{array}{c} -1 \\ 0 \end{array} \right\} k_3 x_1^3(t) + \left\{ \begin{array}{c} -1 \\ 0 \end{array} \right\} k_4 x_1^2(t) + \left\{ \begin{array}{c} -1 \\ 1 \end{array} \right\} k_5 \left(x_1(t) - x_2(t) \right)^3 \tag{23}$$

A zero-mean Gaussian noise is acting on mass *2* so to mimic real conditions where the number of inputs *P* is generally (much) lower than the number of outputs *Q*. The outputs have been corrupted by zero-mean Gaussian noises with rms equal to 6.3% of the outputs rms, roughly corresponding to a 24dB signal-to-noise ratio. The linear estimates – obtained with the same parameters of Table 2 – of the nonlinear system FRFs are plotted in Figure 5, with no added noise. Resonances are right shifted with respect to the natural frequencies f_1=2.463 Hz (damping ratio ζ_1=1.83%) and f_2=7.511 Hz (ζ_2=5.05%.) of the underlying linear system, whose FRFs are also drawn in Figure 5.

The NIPEZ method has been applied in both cases in the frequency range 0–12 Hz with model order 2*n* varying from 2 to 80. Results are summarised in Table 7 and reveal a good accuracy in the estimation of the nonlinear coefficients (k_3, k_4, k_5) and the modal parameters (natural frequencies and damping ratios). As expected the standard deviation is much larger in presence of noise, which is also confirmed by Figure 6 where the trend of the most variable parameter, stiffness k_3, is plotted (black dots). The inspection of the stabilisation diagrams suggests to rely on only a part of the extracted values, i.e. $20<2n<70$ which exhibit a smaller variability, to compute the nonlinear constants.

Table 7 and Figure 6 also present an improved solution, obtained by doubling the number of spectral lines (*M*=8192). This result suggests that a large number of points in the frequency domain is advisable but only if a minimum reasonable number of data block , e.g. 10, is used to compute the mean values involved in the definition of the PSDs in eq.(10).

The inaccuracies on the nonlinear coefficients k_3, k_4, k_5 are comparable with the results in [10] where 2.3%, 1.1% and 1.9% errors are reported in a 2% noise condition. Very accurate damping ratios are again achieved, even in the noisy condition, which distinguishes NIPEZ from NSI [10].

Figure 7 presents the differences between the estimated frequencies and the theoretical values as a function of the model order, with 6.3% noise and *M*=8192 spectral lines. With model order 4, namely ideal for a two degree of freedom system, a maximum error of about 2.3% is present on the second mode frequency; the amplitude (Fig. 5) of the first mode is much larger and the frequency difference is well below 0.5%. The errors then decrease at higher orders, as a consequence of a stable identification. Figure 7, and similar plots valid for the single degree of freedom examples of the previous sections (not presented for the sake of brevity), indicates that the proposed method can

give a correct identification of the linear parameters even with the ideal model order but that stabilisation diagrams are very useful for increasing the accuracy of both linear and nonlinear estimates.

It is important to mention that vectors $\mathbf{b}_{qk}$ are necessary, with $q = 1, \ldots, Q$ and $k = 1, \ldots, N$ (k indicates the input) to compute the nonlinear parameters μ_s from eq.(11). In the present example a single input is present on mass 2, i.e. $k \equiv 2$, and then $\mathbf{b}_{q2}$ vectors only can be determined, q=1,2. Since vectors $\mathbf{b}_{qk}$ are related to the zeros of the underlying linear system – eq.(7) – it's possible to set $\mathbf{b}_{kq} = \mathbf{b}_{qk}$, and then $\mathbf{b}_{2q} = \mathbf{b}_{q2}$, which allows for a correct usage of eq.(11). For example the nonlinear coefficient μ_1 may be evaluated with the following expression

$$\mathbf{d}_{21} = \mu_1 \left(\mathbf{b}_{21} L_{11} + \mathbf{b}_{22} L_{21} \right) = \mu_1 \left(\mathbf{b}_{12} L_{11} + \mathbf{b}_{22} L_{21} \right) \tag{24}$$

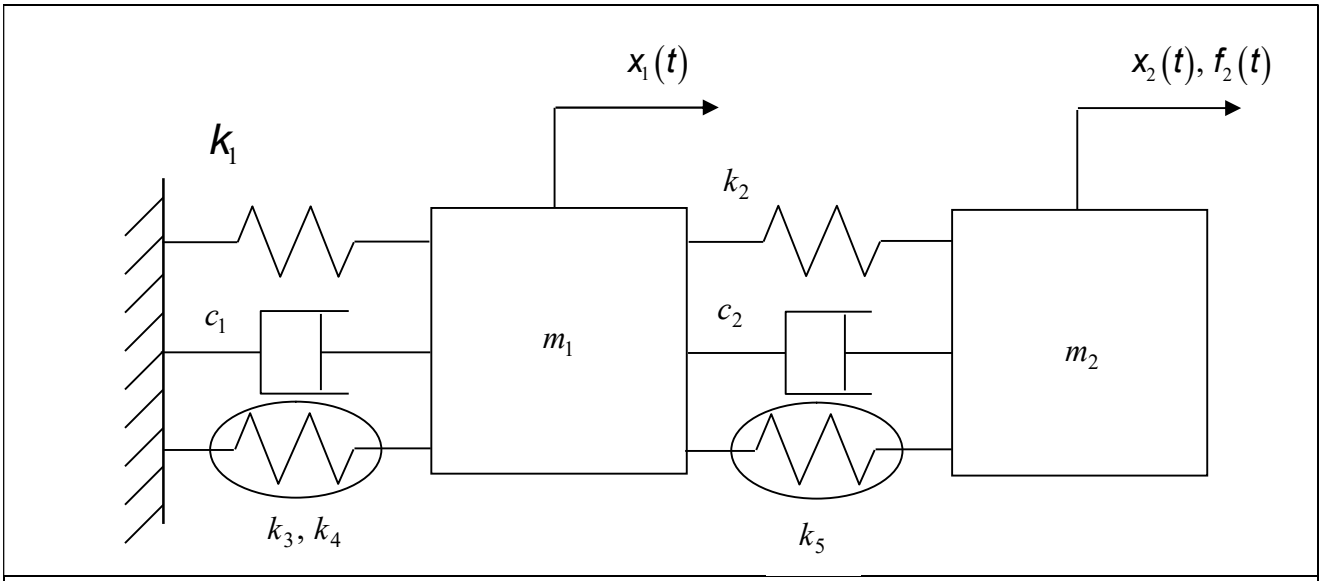

Figure 4: sketch of the two degrees of freedom system

Table 6: parameters of the two degrees of freedom system.

Mass (kg)	Damping (Ns/m)	Linear stiffness (N/m)	Cubic nonlinear stiffness (N/m^3)	Quadratic nonlinear stiffness (N/m^2)
$m_1 = 1.0$	$c_1 = 2.0$	$k_1 = 800$	$k_3 = 8.0 \cdot 10^7$	$k_4 = 8.0 \cdot 10^4$
$m_2 = 1.5$	$c_2 = 2.0$	$k_2 = 1000$	$k_5 = 1.0 \cdot 10^8$	

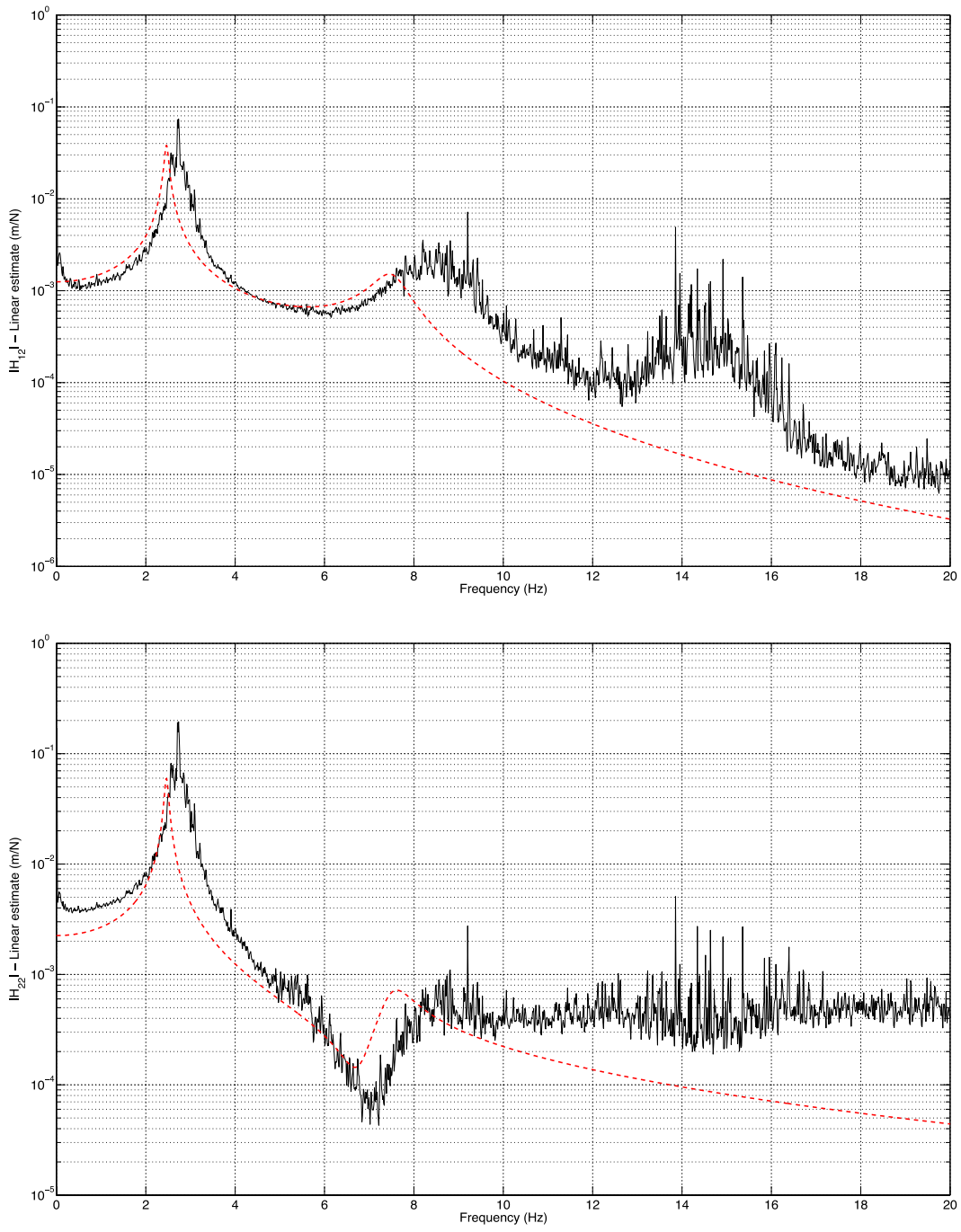

Figure 5: linear estimates (solid lines) of the nonlinear FRFs of the two degrees of freedom system, $\left|H_{12}(\omega)\right|$ (top) and $\left|H_{22}(\omega)\right|$ (bottom). Ideal linear FRFs are represented with dashed lines.

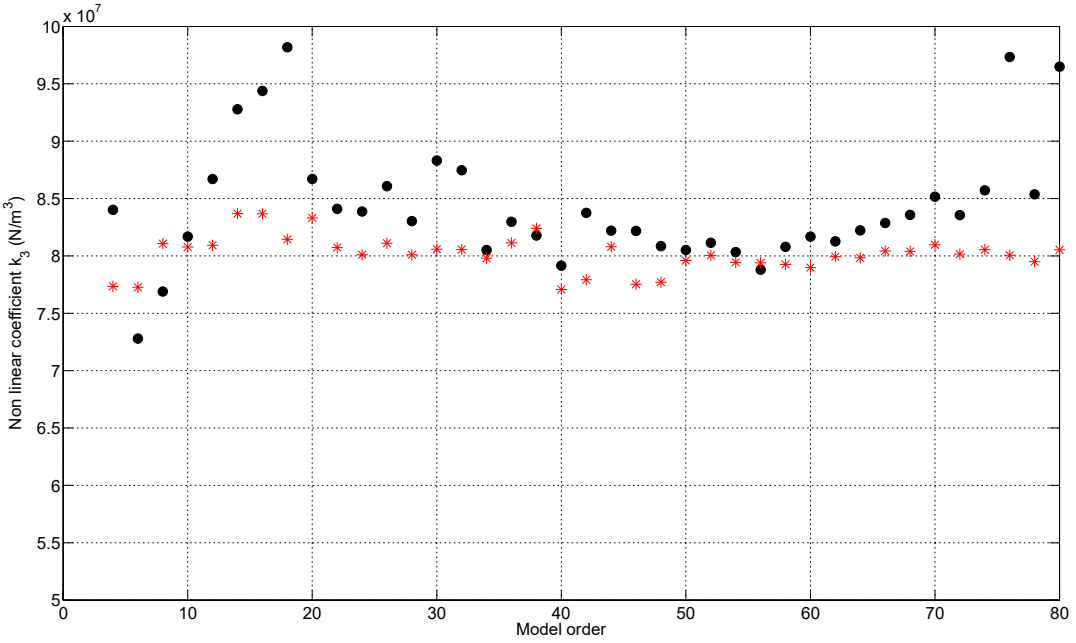

Figure 6: variation of the nonlinear coefficient k_3 with model order, with 6.3% noise.
Spectral lines M=4096: dots •, M=8192: asterisks *.

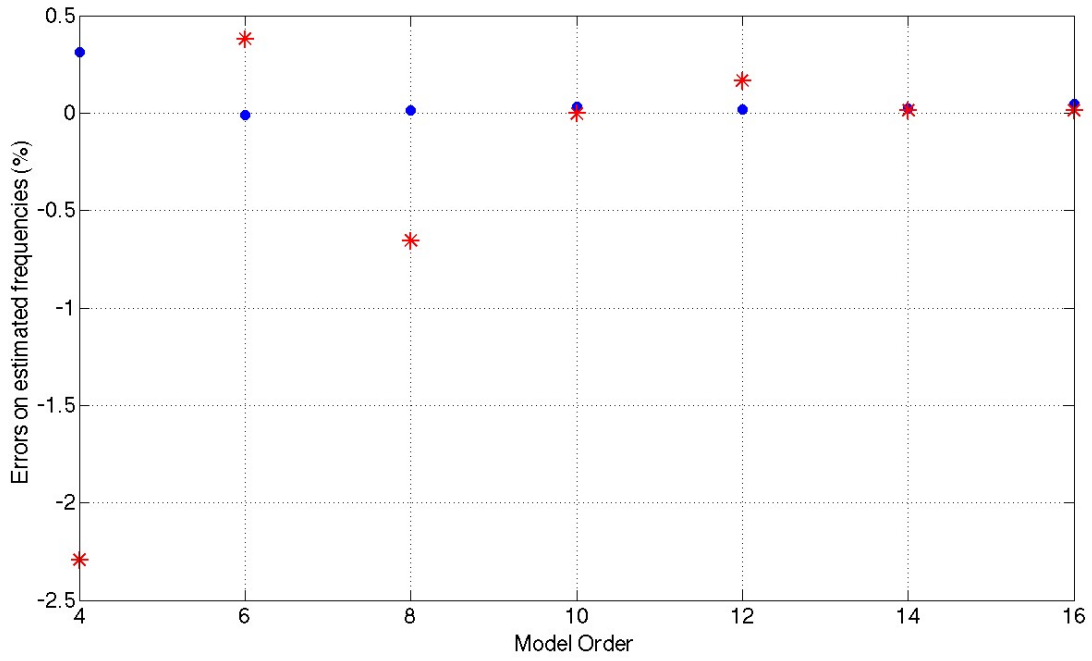

Figure 7: errors on the estimated frequencies with increasing model order, with 6.3% noise and M=8192 spectral lines. o: f_1, *: f_2

Table 7: estimates of linear and nonlinear parameters, without and with noise, in the region $20<2n<80$.

	k_3 (N/m^3)	k_4 (N/m^2)	k_5 (N/m^3)	f_1 (Hz)	ζ_1 (%)	f_2 (Hz)	ζ_2 (%)
Ideal	$8.00\cdot10^7$	$8.00\cdot10^4$	$1.00\cdot10^8$	2.463	1.83	7.511	5.05
M=4096	No noise						
Mean value	$8.13\cdot10^7$	$8.06\cdot10^4$	$1.02\cdot10^8$	2.464	1.89	7.515	5.08
Standard deviation	$2.48\cdot10^5$	$2.10\cdot10^2$	$5.60\cdot10^5$	$8.36\cdot10^{-4}$	$5.2\cdot10^{-2}$	$0.3\cdot10^{-2}$	$2.2\cdot10^{-2}$
M =4096	6.3% noise						
Mean value	$8.22\cdot10^7$	$7.95\cdot10^4$	$1.03\cdot10^8$	2.463	1.75	7.519	5.13
Standard deviation	$2.45\cdot10^6$	$2.48\cdot10^3$	$3.66\cdot10^6$	$0.27\cdot10^{-2}$	0.15	$7.8\cdot10^{-2}$	0.12
M =8192	No noise						
Mean value	$8.13\cdot10^7$	$8.06\cdot10^4$	$1.01\cdot10^8$	2.464	1.87	7.513	5.05
Standard deviation	$1.14\cdot10^5$	$1.25\cdot10^2$	$3.10\cdot10^5$	$6.02\cdot10^{-4}$	$2.64\cdot10^{-2}$	$0.11\cdot10^{-2}$	$1.9\cdot10^{-2}$
M =8192	6.3% noise						
Mean value	$8.01\cdot10^7$	$7.89\cdot10^4$	$1.02\cdot10^8$	2.464	1.79	7.528	5.04
Standard deviation	$1.41\cdot10^6$	$1.03\cdot10^3$	$3.41\cdot10^7$	$8.44\cdot10^{-4}$	$2.69\cdot10^{-2}$	$0.75\cdot10^{-2}$	0.14

Table 8 reports the results achieved by setting M=8192 and limiting the analysis to the frequency band 0–6 Hz, still in the 6.3% noise condition. The first mode only is selected and then it is not possible to get any estimate of the natural frequency and damping ratio of the second mode. It is nonetheless feasible to correctly evaluate the nonlinear terms, with a similar accuracy as in the previous 0–12 Hz band elaboration.

On the contrary no stable solution is determined by selecting the 6–12 Hz band. The result is not surprising taking into consideration – Fig.(5) – that the amplitudes of the FRFs in the second mode region are at least one order of magnitude lower than the corresponding amplitudes of the first mode.

Table 8: estimates of linear and nonlinear parameters, with 6.3% noise, M=8192, in the 0–6 Hz band.

	k_3 (N/m^3)	k_4 (N/m^2)	k_5 (N/m^3)	f_1 (Hz)	ζ_1 (%)	f_2 (Hz)	ζ_2 (%)
Mean value	$7.98\cdot10^7$	$7.91\cdot10^4$	$1.05\cdot10^8$	2.464	1.81	–	–
Standard deviation	$1.17\cdot10^6$	$1.19\cdot10^3$	$4.19\cdot10^6$	$9.44\cdot10^{-4}$	0.04	–	–

4. Conclusions

The paper presents a frequency domain procedure aiming at the synchronous identification of the nonlinear coefficients and the modal parameters of a MIMO system described by second order differential equations. A z-domain polynomial expansion of the underlying linear FRFs is incorporated into the identification process leading to an overdetermined linear system of algebraic equations. A least squares analytical solution of this latter problem is outlined, which is indeed necessary both to limit the data processing time and to increase the stability of the numerical solution.

Numerical examples are given to show the correctness of the method, which actually attains very good results for both the linear and nonlinear parameters, even in presence of noise. The stabilisation diagram of the nonlinear coefficients revels very useful to define their true values and also makes it clear that the model order ($2n$) corresponding to twice the actual number of degrees of freedom is not an appropriate choice to identify the nonlinear parameters. The standard deviation of the coefficients, computed with $2n$ varying between a minimum and a maximum value, results to be a good indicator of the quality of the estimates, both linear and nonlinear.

One of the merits of NIPEZ is the capability of extracting modal parameters and nonlinear coefficients simultaneously (even with non negligible noise levels), which allows to verify if all the parameters converge to reliable estimates. In particular numerical simulations lead to very precise and low scattered damping ratios, which are usually difficult to obtain.

The computational burden is very limited, mainly thanks to the least square procedure developed in Appendix A: all the results herewith presented have been obtained in few tens of seconds with Matlab® R2011a, on a 1.7 GHz Core i5 processor and 4 GB ram memory.

Very long input and output time histories can simply be handled, and are even appreciated, since they're quickly transformed in the frequency domain at the very beginning of the procedure; conversely too short time series may lead to an unsatisfactory frequency resolution and a consequently imperfect identification. This characteristic makes the proposed method somehow complementary to the previously developed time domain technique NSI [10] which has to limit the number of measured samples to avoid computational memory issues but can produce accurate results also with short time data sets. Also the possibility of arbitrarily setting the frequency band of analysis can somehow be seen as an advantage over time domain methods, although an incorrect decision on the frequency range can lead to inaccurate results.

Gaussian random input has been imposed in the proposed numerical examples, so that proper choice of windows and overlap was mandatory; periodic random input could avoid both these selections but numerical examples showed that this assumption is not compulsory.

The main drawback of the described procedure is intrinsic to its formulation: in eq. (1) one has to know the number and location of nonlinearities to correctly express the equations of motion and also has to assume appropriate functions (e.g. cubic stiffness) and, sometimes, parameters (e.g. clearance) to describe the behaviour of nonlinear forces. The evaluation of the model order can be seen as a weakness of the method, which in fact generates unsatisfactory results on the nonlinear coefficients if the theoretical model order is used, although this limitation is not so severe when the linear parameters are considered. We stress the importance of using stabilization diagrams, and present results with both mean values and standard deviations for linear and nonlinear terms.

Future work should address to the examination of the PSD related parameters (number of spectral lines and averages), mostly to limit the variability of the estimates caused by noise. A certain attention should also be dedicated to the influence of the frequency band of analysis and the kind of input, the latter in relation to the choice of the window function and the influence of harmonic components. A more accurate survey of the properties of stabilisation diagrams could also lead to an objective, automatic and reliable selection of the model order, based on all the identified information. Finally an application to real data and an extensive comparison with other techniques will certainly be compulsory.

References

[1] G. Kerschen, K. Worden, A.F. Vakakis, J.-C. Golinval, Past, present and future of nonlinear system identification in structural dynamics, Mechanical Systems and Signal Processing 20 (2006), pp. 505-592

[2] S.A. Billings, Nonlinear system identification: NARMAX methods in the time, frequency, and spatio-temporal domains, Wiley, 2013

[3] L. Ljung, Perspectives on system identification, Annual Reviews in Control 34 (2010), pp. 1–12

[4] O. Nelles, Nonlinear system identification. From classical approaches to neural networks and fuzzy models, Springer, 2001

[5] M. Feldman, Hilbert transform methods for nonparametric identification of nonlinear time varying vibration systems, Mechanical Systems and Signal Processing 47 (2014), pp. 66-77

[6] A. Marconato, J. Sjoberg, J. Suykens, J. Schoukens, Identification of the Silverbox benchmark using nonlinear state-space models, 16th IFAC Symposium on System Identification, July 11-13, 2012

[7] B. Zhang, S.A. Billings, Identification of continuous-time nonlinear systems: The nonlinear difference equation with moving average noise (NDEMA) framework , Mechanical Systems and Signal Processing 60–61 (2015), pp. 810–835

[8] V. Verdult, Nonlinear system identification: a state-space approach, PhD thesis, University of Twente, 2002

[9] A.C. Gondhalekar, Strategies for non linear system identification, PhD thesis, Imperial College London, 2009

[10] S. Marchesiello, L. Garibaldi, A time domain approach for identifying nonlinear vibrating structures by subspace methods, Mechanical Systems and Signal Processing 22 (2008), pp. 81-101

[11] J.P. Noël, G. Kerschen, Frequency-domain subspace identification for nonlinear mechanical systems, Mechanical Systems and Signal Processing 40 (2013), pp. 701–717

[12] J.P. Noël, S. Marchesiello, G. Kerschen, Subspace-based identification of a nonlinear spacecraft in the time and frequency domains, Mechanical Systems and Signal Processing 43 (2014), pp. 217–236

[13] D.E. Adams, R.J. Allemang, A frequency domain method for estimating the parameters of a non-linear structural dynamic model through feedback, Mechanical Systems and Signal Processing 14 (2000), pp. 637-656.

[14] K. Shin, J.K. Hammond, Fundamentals of Signal Processing for Sound and Vibration Engineers, Wiley, 2008

[15] A. Fasana, Modal parameters estimation in the *z*-domain, Mechanical Systems and Signal Processing 23 (2009), pp. 217-225

[16] P. Verboven, Frequency-domain system identification for modal analysis, Ph.D. thesis, Vrije Universiteit Brussel, 2002

[17] B. Cauberghe, Applied frequency-domain system identification in the field of experimental and operational modal analysis, Ph.D. thesis, Vrije Universiteit Brussel, 2004

Appendix A

The algebraic passages that lead to the least squares solution given by eq.(17) are detailed in this section. The linear equation for generic output q, eq.(13), is

$$\mathbf{A}_q\mathbf{a}+\sum_{p=1}^{P}\mathbf{B}_{qp}\,\mathbf{b}_{qp}+\sum_{s=1}^{S}\mathbf{D}_{qs}\mathbf{d}_{qs}+\mathbf{n}_q=\mathbf{e}_q \tag{A.1}$$

where $\mathbf{e}_q$ is the error vector and $\mathbf{a}$, $\mathbf{b}_{qp}$ and $\mathbf{d}_{qs}$ are to be determined, for a total of $1+Q\cdot P+Q\cdot S$ unknown vectors. The real valued scalar error $E_q^2=\mathbf{e}_q^H\mathbf{e}_q$ (^{H} indicates the Hermitian transpose) is one of the elements of the global error E^2, which takes into account all the Q outputs

$$E^2=\sum_{q=1}^{Q}E_q^2=\sum_{q=1}^{Q}\left(\mathbf{a}^H\mathbf{A}_q^H+\sum_{p=1}^{P}\mathbf{b}_{qp}^H\mathbf{B}_{qp}^H+\sum_{s=1}^{S}\mathbf{d}_{qs}^H\mathbf{D}_{qs}^H+\mathbf{n}_q^H\right)\left(\mathbf{A}_q\mathbf{a}+\sum_{p=1}^{P}\mathbf{B}_{qp}\,\mathbf{b}_{qp}+\sum_{s=1}^{S}\mathbf{D}_{qs}\mathbf{d}_{qs}+\mathbf{n}_q\right) \tag{A.2}$$

With the aim of minimising E^2, partial derivatives with respect to vectors $\mathbf{a}$, $\mathbf{b}_{qp}$ and $\mathbf{d}_{qs}$ are set to zero, i.e.

$$\begin{cases}\partial E^2/\partial\mathbf{a}=0\\ \partial E^2/\partial\mathbf{b}_{qp}=0 \quad \text{with} \quad q=1,\dots,Q;\quad p=1,\dots,P\\ \partial E^2/\partial\mathbf{d}_{qs}=0 \qquad\qquad q=1,\dots,Q;\quad s=1,\dots,S\end{cases} \tag{A.3}$$

By remembering that the partial derivative of a matrix product gives

$$\begin{aligned}\partial\left(\mathbf{x}^H\mathbf{Y}\,\mathbf{z}\right)/\partial\mathbf{x}&=\mathbf{Y}\,\mathbf{z}\\ \partial\left(\mathbf{x}^H\mathbf{Y}\,\mathbf{z}\right)/\partial\mathbf{z}&=\mathbf{Y}\,\mathbf{x}\end{aligned} \tag{A.4}$$

we can also recognise that

$$\partial\left(\mathbf{x}^H\mathbf{Y}^H\mathbf{Y}\,\mathbf{x}\right)/\partial\mathbf{x}=2\mathbf{Y}^H\mathbf{Y}\,\mathbf{x} \tag{A.5}$$

The last equation displays the typical structure occurring when performing the products of eq.(A.2) and the subsequent derivatives; eq.(A.3) then reads

$$\begin{cases}\sum_{q=1}^{Q}\mathbf{A}_q^H\mathbf{R}_q=0\\ \mathbf{B}_{qp}^H\mathbf{R}_q=0 \quad \text{with} \quad q=1,\dots,Q;\quad p=1,\dots,P\\ \mathbf{D}_{qs}^H\mathbf{R}_q=0 \qquad\qquad q=1,\dots,Q;\quad s=1,\dots,S\end{cases} \tag{A.6}$$

where $\mathbf{R}_q=\mathbf{A}_q\mathbf{a}+\mathbf{B}_{q1}\,\mathbf{b}_{q1}+\dots+\mathbf{B}_{qP}\,\mathbf{b}_{qP}+\mathbf{D}_{q1}\mathbf{d}_{q1}+\dots+\mathbf{D}_{qS}\mathbf{d}_{qS}+\mathbf{n}_q$

By highlighting the unknown vectors $\mathbf{a}$, $\mathbf{b}_{qp}$ and $\mathbf{d}_{qs}$, eq.(A.6) gives $\mathbf{S}\mathbf{x}=\mathbf{m}$ – eq.(17) – with

$$\mathbf{S}=\begin{bmatrix}
\sum_{q=1}^{Q}\mathbf{A}_q^H\mathbf{A}_q & \mathbf{A}_1^H\mathbf{B}_{11} & \cdots & \mathbf{A}_Q^H\mathbf{B}_{Q1} & \cdots & \mathbf{A}_1^H\mathbf{B}_{1P} & \cdots & \mathbf{A}_Q^H\mathbf{B}_{QP} & \mathbf{A}_1^H\mathbf{D}_{11} & \cdots & \mathbf{A}_Q^H\mathbf{D}_{Q1} & \cdots & \mathbf{A}_1^H\mathbf{D}_{1S} & \cdots & \mathbf{A}_Q^H\mathbf{D}_{QS} \\
\mathbf{B}_{11}^H\mathbf{A}_1 & \mathbf{B}_{11}^H\mathbf{B}_{11} & \cdots & 0 & \cdots & \mathbf{B}_{11}^H\mathbf{B}_{1P} & \cdots & 0 & \mathbf{B}_{11}^H\mathbf{D}_{11} & \cdots & 0 & \cdots & \mathbf{B}_{11}^H\mathbf{D}_{1S} & \cdots & 0 \\
\vdots & \vdots & \ddots & \vdots & \cdots & \vdots & \ddots & \vdots & \vdots & \ddots & \vdots & \cdots & \vdots & \ddots & \vdots \\
\mathbf{B}_{Q1}^H\mathbf{A}_Q & 0 & \cdots & \mathbf{B}_{Q1}^H\mathbf{B}_{Q1} & \cdots & 0 & \cdots & \mathbf{B}_{Q1}^H\mathbf{B}_{QP} & 0 & \cdots & \mathbf{B}_{Q1}^H\mathbf{D}_{Q1} & \cdots & 0 & \cdots & \mathbf{B}_{Q1}^H\mathbf{D}_{QS} \\
\vdots & \vdots & \cdots & \vdots & \cdots & \vdots & \cdots & \vdots & \vdots & \cdots & \vdots & \cdots & \vdots & \cdots & \vdots \\
\mathbf{B}_{1P}^H\mathbf{A}_1 & \mathbf{B}_{1P}^H\mathbf{B}_{11} & \cdots & 0 & \cdots & \mathbf{B}_{1P}^H\mathbf{B}_{1P} & \cdots & 0 & \mathbf{B}_{1P}^H\mathbf{D}_{11} & \cdots & 0 & \cdots & \mathbf{B}_{1P}^H\mathbf{D}_{1S} & \cdots & 0 \\
\vdots & \vdots & \ddots & \vdots & \cdots & \vdots & \ddots & \vdots & \vdots & \ddots & \vdots & \cdots & \vdots & \ddots & \vdots \\
\mathbf{B}_{QP}^H\mathbf{A}_Q & 0 & \cdots & \mathbf{B}_{QP}^H\mathbf{B}_{Q1} & \cdots & 0 & \cdots & \mathbf{B}_{QP}^H\mathbf{B}_{QP} & 0 & \cdots & \mathbf{B}_{QP}^H\mathbf{D}_{Q1} & \cdots & 0 & \cdots & \mathbf{B}_{QP}^H\mathbf{D}_{QS} \\
\mathbf{D}_{11}^H\mathbf{A}_1 & \mathbf{D}_{11}^H\mathbf{B}_{11} & \cdots & 0 & \cdots & \mathbf{D}_{11}^H\mathbf{B}_{1P} & \cdots & 0 & \mathbf{D}_{11}^H\mathbf{D}_{11} & \cdots & 0 & \cdots & \mathbf{D}_{11}^H\mathbf{D}_{1S} & \cdots & 0 \\
\vdots & \vdots & \ddots & \vdots & \cdots & \vdots & \ddots & \vdots & \vdots & \ddots & \vdots & \cdots & \vdots & \ddots & \vdots \\
\mathbf{D}_{Q1}^H\mathbf{A}_Q & 0 & \cdots & \mathbf{D}_{Q1}^H\mathbf{B}_{Q1} & \cdots & 0 & \cdots & \mathbf{D}_{Q1}^H\mathbf{B}_{QP} & 0 & \cdots & \mathbf{D}_{Q1}^H\mathbf{D}_{Q1} & \cdots & 0 & \cdots & \mathbf{D}_{Q1}^H\mathbf{D}_{QS} \\
\vdots & \vdots & \cdots & \vdots & \cdots & \vdots & \cdots & \vdots & \vdots & \cdots & \vdots & \cdots & \vdots & \cdots & \vdots \\
\mathbf{D}_{1S}^H\mathbf{A}_1 & \mathbf{D}_{1S}^H\mathbf{B}_{11} & \cdots & 0 & \cdots & \mathbf{D}_{1S}^H\mathbf{B}_{1P} & \cdots & 0 & \mathbf{D}_{1S}^H\mathbf{D}_{11} & \cdots & 0 & \cdots & \mathbf{D}_{1S}^H\mathbf{D}_{1S} & \cdots & 0 \\
\vdots & \vdots & \ddots & \vdots & \cdots & \vdots & \ddots & \vdots & \vdots & \ddots & \vdots & \cdots & \vdots & \ddots & \vdots \\
\mathbf{D}_{QS}^H\mathbf{A}_Q & 0 & \cdots & \mathbf{D}_{QS}^H\mathbf{B}_{Q1} & \cdots & 0 & \cdots & \mathbf{D}_{QS}^H\mathbf{B}_{QP} & 0 & \cdots & \mathbf{D}_{QS}^H\mathbf{D}_{Q1} & \cdots & 0 & \cdots & \mathbf{D}_{QS}^H\mathbf{D}_{QS}
\end{bmatrix}$$

$$\mathbf{x}^T=\begin{bmatrix}\mathbf{a} & \mathbf{b}_{11} & \cdots & \mathbf{b}_{Q1} & \cdots & \mathbf{b}_{1P} & \cdots & \mathbf{b}_{QP} & \mathbf{d}_{11} & \cdots & \mathbf{d}_{Q1} & \cdots & \mathbf{d}_{1S} & \cdots & \mathbf{d}_{QS}\end{bmatrix}$$

$$\mathbf{m}^T=-\begin{bmatrix}\sum_{q=1}^{Q}\mathbf{A}_q^H\mathbf{n}_q & \mathbf{B}_{11}^H\mathbf{n}_1 & \cdots & \mathbf{B}_{Q1}^H\mathbf{n}_Q & \cdots & \mathbf{B}_{1P}^H\mathbf{n}_1 & \cdots & \mathbf{B}_{QP}^H\mathbf{n}_Q & \mathbf{D}_{11}^H\mathbf{n}_1 & \cdots & \mathbf{D}_{Q1}^H\mathbf{n}_Q & \cdots & \mathbf{D}_{1S}^H\mathbf{n}_1 & \cdots & \mathbf{D}_{QS}^H\mathbf{n}_Q\end{bmatrix}$$